Available online at www.sciencedirect.com
ScienceDirect
Journal of Sound and Vibration 298 (2006) 404–419
JOURNAL OF SOUND AND VIBRATION
www.elsevier.com/locate/jsvi

# Bending vibration of perforated beams in contact with a liquid

Kyeong-Hoon Jeong[a,*], Marco Amabili[b]

[a]*Mechanical Engineering Division, Korea Atomic Energy Research Institute, P.O. Box 105, Yuseong, Daejeon 305-600, Republic of Korea*
[b]*Department of Industrial Engineering, University of Parma, Parco Area delle Scienze 181/A, 43100 Parma, Italy*

Received 5 December 2005; received in revised form 28 March 2006; accepted 29 May 2006
Available online 31 July 2006

**Abstract**

A theoretical study on the natural frequencies and the mode shapes of perforated beams in contact with an ideal liquid is presented. In the theory part, it is assumed that the beams are simply supported at both ends and the ideal liquid is in contact with the lower surface of the beams. Holes with an identical configuration are equally spaced in the beams and three specific patterns of square, rotated square and circular holes are considered. Along the contact surface between the beam and the liquid, the compatibility requirement is applied for the liquid–structure interaction and the Rayleigh–Ritz method is used to calculate the eigenvalues and eigenvectors of the system. The proposed theoretical method for the beams coupled with the liquid is verified by observing a good agreement with the three-dimensional finite element analysis results. In order to evaluate the dynamic characteristics of the liquid-coupled beam, the effects of the hole size in the beams and the pattern of holes on the natural frequencies and the mode shapes are investigated. Additionally the effects of the liquid depth on the natural frequency is investigated and compared with the solid beam case.


## 1. Introduction

A structure, which is constructed by repeating a basic geometric unit to form a regular pattern, is known as a periodic structure. Periodic structures can be analyzed most efficiently when the periodicity is taken into account. This allows for the behavior of the complete structure to be determined through an analysis of the basic unit. The substitute continuum approach is based on the global behavior of the structure by using the effective Poisson's ratio and the effective modulus of the elasticity. One of the periodic structures is a perforated structure, which has a number of identical circular holes or square holes with a regular pattern.

The perforated plates with a number of circular holes are used not only in commercial nuclear power plants but also in heat exchangers. However, it is very difficult to estimate the dynamic characteristics of such a perforated plate. Moreover, the dynamic behavior of perforated plates in contact with a liquid is very complicated due to the fluid–structure interaction. Although, powerful numerical tools such as the finite element method or the boundary element method make numerical solutions to a simple fluid–structure interaction problem possible, the use of these methods in perforated structures still requires enormous

*Corresponding author. Tel.: +82 42 868 8792.
*E-mail address:* khjeong@kaeri.re.kr (K.-H. Jeong).

0022-460X/$ - see front matter © 2006 Elsevier Ltd. All rights reserved.
doi:10.1016/j.jsv.2006.05.029

amounts of time for a modeling and computation. In particular, the coupling between a structure and a liquid in a finite element modeling requires elaborate modeling techniques and an understanding of the physical phenomena in the fluid–structure interaction.

The previous studies on perforated plates have been focused on the stress distribution and the deformation based on the effective elastic constants such as the effective Young's modulus, the effective Poisson's ratio and the effective mass density [1–5]. In these studies, the theories and observations were based on the static deformation and stress calculation of the perforated plates. There have been several applications of the effective elastic constants for perforated plates. De Santo [6] carried out an experimental modal analysis of perforated circular plates. However, it was inappropriate to use the equivalent elastic properties since the holes in the plates were too large when compared with the plate dimensions. Burgemeister and Hansen [7] suggested a formula to estimate the effective resonance frequencies of rectangular plates in air, based on finite element analysis and experiments. Jeong et al. [8] carried out an experimental modal analysis for perforated plates in contact with a fluid. They showed that the natural frequencies of the clamped perforated plates in air could be predicted by using the equivalent elastic properties. Sinha et al. [9] attempted to estimate the added mass of submerged perforated plates by conducting a modal test and finite element analysis.

However, the theoretical method based on the averaged elastic constants can produce some deviations in the higher vibration modes of perforated plates. Especially, when the perforated plates have only a few holes, the equivalent elastic constant is not effective any more; therefore an application of this method will be limited. Although the holes are distributed evenly in the plates, the effective elastic constants of the perforated plates, strictly speaking, will be a function of the mode shapes.

Since very few studies on the theoretical dynamic analysis of a liquid-coupled perforated beam have been undertaken, this paper will suggest a theoretical method to estimate the natural frequencies and mode shapes of perforated beams not only in air but also in contact with a liquid. This method can be effectively used to verify the finite element dynamic analyses such as the seismic analysis and the postulated pipe break analysis of the reactor internals of a nuclear power plant.

## 2. Theoretical formulation

### 2.1. Distributed properties of elastic perforated beams

Liquid-contacting beams having several identical holes at the same distance are illustrated in Fig. 1. The simply supported beam has a total length $L$, thickness $h$, width $b$, diameter of the circular holes $d$, or width of the square holes $s$. The beams are composed of $N$ element regions with the width of $a$. Since the square holes of the beam are equally spaced, the distributed mass in the $n$th element region of a beam can be written as

$$v(x) = \begin{cases} \rho b, & na \leqslant x < na + a_1, \\ \rho(b-s), & na + a_1 \leqslant x < n\,a + a_2, \\ \rho b, & na + a_2 \leqslant x < (n+1)a, \end{cases} \tag{1}$$

where $a_1 = (a-s)/2$, $a_2 = (a+s)/2$ and $\rho$ is the density of the beam. Similarly, the area moment of inertia distribution of the $n$th element region of the perforated beam becomes

$$I(x) = \begin{cases} bh^3/12, & na \leqslant x < na + a_1, \\ (b-s)h^3/12, & na + a_1 \leqslant x < na + a_2, \\ bh^3/12, & na + a_2 \leqslant x < (n+1)a. \end{cases} \tag{2}$$

The rotated square holes of the beam have identical dimensions and are located in a row with an equal space, therefore the distributed mass and the moment of inertia distributions in the $n$th element region

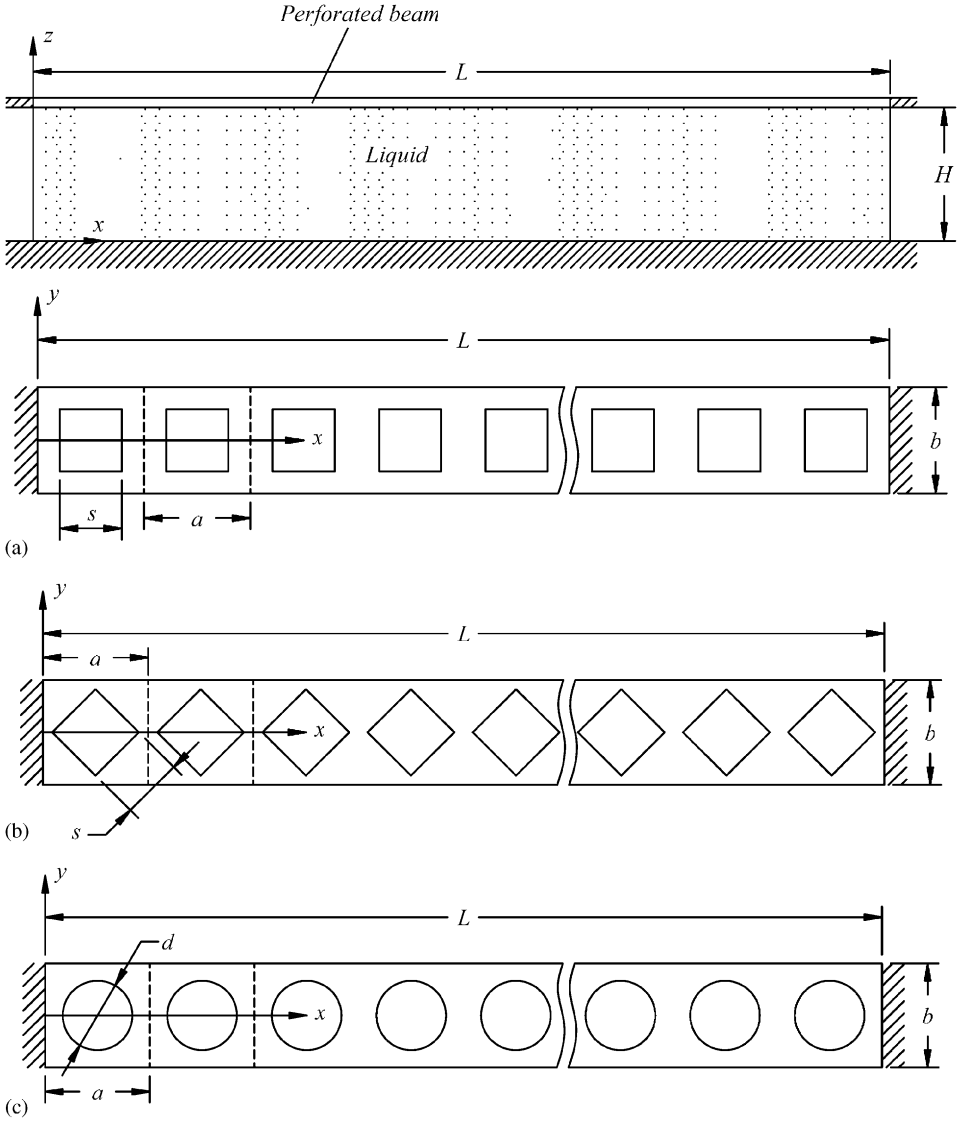


Fig. 1. Perforated beams in contact with a liquid: (a) perforated beam with square holes, (b) perforated beam with rotated square holes and (c) perforated beam with circular holes.

can be given as

$$v(x) = \begin{cases} \rho b, & na \leqslant x < na + a_3, \\ \rho(b + 2na + 2a_3 - 2x), & na + a_3 \leqslant x < na + a/2, \\ \rho(b - 2na - 2a_4 + 2x), & na + a/2 \leqslant x < na + a_4, \\ \rho b, & na + a_4 \leqslant x < (n+1)a, \end{cases} \tag{3}$$

$$I(x) = \begin{cases} bh^3/12, & na \leqslant x < na + a_3, \\ (b + 2na + 2a_3 - 2x)h^3/12, & na + a_3 \leqslant x < na + a/2, \\ (b - 2na - 2a_4 + 2x)h^3/12, & na + a/2 \leqslant x < na + a_4, \\ bh^3/12, & na + a_4/2 \leqslant x < (n+1)a, \end{cases} \tag{4}$$

where $a_3 = (a - \sqrt{2}s)/2$ and $a_4 = (a + \sqrt{2}s)/2$. For the perforated beam with circular holes, the distributed mass and the moment of inertia distribution in the $n$th element region of the beam can be obtained as follows:

$$v(x) = \begin{cases} \rho b, & na \leqslant x < na + a_5, \\ \rho\left\{b - \sqrt{d^2 - (2x - 2na - a)^2}\right\}, & na + a_5 \leqslant x < na + a_6, \\ \rho b, & na + a_6 \leqslant x < (n+1)a, \end{cases} \tag{5}$$

$$I(x) = \begin{cases} bh^3/12, & na \leqslant x < na + a_5, \\ \left\{b - \sqrt{d^2 - (2x - 2na - a)^2}\right\}h^3/12, & na + a_5 \leqslant x < na + a_6, \\ bh^3/12, & na + a_6 \leqslant x < (n+1)a, \end{cases} \tag{6}$$

where $a_5 = (a-d)/2$ and $a_6 = (a+d)/2$.

### 2.2. Rayleigh–Ritz method for perforated beams in air

Each dry mode shape in a bending can be approximated by a combination of a finite number of admissible functions, $W_m(x)$ and appropriate unknown coefficients $q_m$. The choice of the admissible functions is very important to simplify the calculations and to guarantee a convergence to the actual solution. The transverse dynamic displacement due to a bending moment, $w$, can be assumed in the form of

$$w(x,t) = \sum_{m=1}^{M} q_m W_m(x) \exp(\mathrm{i}\omega t), \tag{7}$$

where $\mathrm{i} = \sqrt{-1}$ and $\omega$ is the circular natural frequency of the beams. When we consider the geometric boundary conditions at $x = 0$ and $L$, the bending moment and the displacement at both support ends must be zero simultaneously for the simply supported boundary condition, that is

$$M(x)\big|_{x=0} = W_m(x)\big|_{x=0} = M(x)\big|_{x=L} = W_m(x)\big|_{x=L} = 0. \tag{8}$$

The admissible functions for the bending mode can be defined by

$$W_m(x) = \sin\left(\frac{m\pi x}{L}\right). \tag{9}$$

These simple functions are a set of dry modal functions of a uniform beam which satisfies the geometric and natural boundary conditions of Eq. (8).

The Rayleigh–Ritz method is introduced to obtain the natural frequencies and mode shapes of the perforated beams in air. A sufficiently large number of terms, $M$, must be considered and a vector $\mathbf{q}$ of the unknown parameters and a vector of admissible functions $\mathbf{W}$ are introduced in order to perform a numerical calculation

$$\mathbf{q} = \{q_1 \quad q_2 \quad q_3 \cdots q_M\}^{\mathrm{T}}, \tag{10}$$

$$\mathbf{W}(x) = \{W_1 \quad W_2 \quad W_3 \quad \cdots \quad W_M\}^{\mathrm{T}}. \tag{11}$$

Now, it is necessary to know the reference kinetic energy of the beams to calculate the natural frequencies in air. The reference kinetic energy of a simply supported perforated beam can be computed by using the orthogonality of modal displacements:

$$T_b^* = \frac{1}{2}\int_0^L v(x)\mathbf{q}^{\mathrm{T}}\mathbf{W}(x)^{\mathrm{T}}\mathbf{W}(x)\mathbf{q}\,\mathrm{d}x = \frac{1}{2}\mathbf{q}^{\mathrm{T}}\mathbf{Z}\mathbf{q}, \tag{12}$$

where $\mathbf{Z}$ is an $M \times M$ symmetric matrix for the beam with square holes and is given as

$$Z_{jk} = h\sum_{n=0}^{N-1}\int_{na}^{(n+1)a} v(x)W_j(x)W_k(x)\,\mathrm{d}x = \rho h U_{jk} \quad (j,k = 1,2,\ldots M), \tag{13}$$

where

$$U_{jk} = \delta_{jk} b\int_0^L \{W_k(x)\}^2\,\mathrm{d}x - s\sum_{n=0}^{N-1}\int_{na+a_1}^{na+a_2} W_j(x)W_k(x)\,\mathrm{d}x \tag{14}$$

and $\delta_{jk}$ is the Kronecker delta. If $j = k$

$$U_{kk} = \frac{bL}{2} - s\sum_{n=0}^{N-1}\left\{\frac{s}{2} - \left(\frac{L}{2\pi k}\right)\cos\left(\frac{k\pi a}{L}\right)\sin\left(\frac{k\pi s}{L}\right)\right\} \tag{15}$$

for $j \neq k$

$$U_{jk} = \frac{bL}{2}\delta_{jk} - \frac{2sL}{\pi}\sum_{n=0}^{N-1}\left\{\cos\left(\frac{(j-k)(n+1/2)a\pi}{L}\right)\sin\left(\frac{(j-k)s\pi}{2L}\right)\right\}\left(\frac{k}{j^2-k^2}\right). \tag{16}$$

For the beam with rotated square holes, the matrix $\mathbf{U}$ will become

$$\begin{aligned} U_{jk} = {} & \delta_{jk} b\int_0^L \{W_k(x)\}^2\,\mathrm{d}x \\ & - 2\sum_{n=0}^{N-1}\left\{\int_{na+a_3}^{na+a/2}(x - na - a_3)W_j(x)W_k(x)\,\mathrm{d}x + \int_{na+a/2}^{na+a_4}(a_4 + na - x)W_j(x)W_k(x)\,\mathrm{d}x\right\}, \end{aligned} \tag{17}$$

and can be obtained by an integration in a closed form. For the beam with circular holes, the matrix $\mathbf{U}$ will be given by

$$U_{jk} = \delta_{jk} b\int_0^L \{W_k(x)\}^2\,\mathrm{d}x - \sum_{n=0}^{N-1}\int_{na+a_5}^{na+a_6}\sqrt{d^2 - 4(x - na - a/2)^2}\,W_j(x)W_k(x)\,\mathrm{d}x. \tag{18}$$

The maximum strain energy of the perforated beam can be computed by integrating the derivative of the admissible modal functions as

$$V_b = \frac{1}{2}\int_0^L EI(x)\mathbf{q}^{\mathrm{T}}\left(\frac{\partial^2\mathbf{W}^{\mathrm{T}}}{\partial x^2}\right)\left(\frac{\partial^2\mathbf{W}}{\partial x^2}\right)\mathbf{q}\,\mathrm{d}x = \frac{1}{2}\mathbf{q}^{\mathrm{T}}\mathbf{S}\mathbf{q}, \tag{19}$$

where $E$ is the modulus of the elasticity of the beams. By inserting the derivatives of the admissible modal functions into Eq. (19), the maximum strain energy of the perforated beam with square holes is obtained by

$$\begin{aligned} S_{jk} &= E\sum_{n=0}^{N-1}\int_{na}^{(n+1)a} I(x)\{W_j(x)''\}\{W_k(x)''\}\,\mathrm{d}x \\ &= \frac{Eh^3}{12}\left[b\delta_{jk}\int_0^L \{W_k(x)''\}^2\,\mathrm{d}x - s\sum_{n=0}^{N-1}\int_{na+a_1}^{na+a_2}\{W_j(x)''\}\{W_k(x)''\}\,\mathrm{d}x\right], \end{aligned} \tag{20}$$

where the symbol $''$ has been used instead of $\mathrm{d}^2/\mathrm{d}x^2$. By inserting Eq. (9) into Eq. (20), it gives

$$S_{jk} = \frac{Eh^3k^2j^2\pi^4}{12L^4}U_{jk}, \tag{21}$$

Similary, the matrix can be obtained for the beams with the rotated square holes or with the circular holes in the same manner as Eq. (21). Since the Rayleigh quotient for the beam vibration in air is given as $V_b/T_b^*$, the matrix equation of an eigenvalue problem can be obtained by minimizing the Rayleigh quotient with respect to the unknown parameters $\mathbf{q}$:

$$\mathbf{S}\mathbf{q} - \omega^2\mathbf{Z}\mathbf{q} = \{0\}. \tag{22}$$

From Eq. (22), the natural frequencies and the mode shapes of the perforated beams in air can be obtained.

### 2.3. Method of a solution for a perforated beam in contact with a liquid

The oscillatory motion of an incompressible and inviscid liquid in contact with a perforated beam can be described by using the velocity potential. It is assumed that the ideal liquid is bounded at the lower bottom by a rigid surface and both ends of a liquid in the $x$ direction have a zero pressure (at $x = 0, L$, see Fig. 1). The liquid surface at the holes is also assumed to be bounded. In fact, the liquid domain is assumed to be two dimensional, and the liquid motion is neglected. This is obviously an approximation. In an actual condition, the liquid at the holes can present: either a free surface where a sloshing is possible, or it can be constrained by a cylindrical surface in the case of pipes which are inserted into the holes and immersed into the liquid. The liquid movement induced by the beam vibration should satisfy the Laplace equation

$$\nabla^2 \Phi(x, z, t) = 0. \tag{23}$$

When the harmonic time function is assumed, the velocity function $\Phi$ can be separated with respect to $z$ in terms of the displacement potential function $\phi(x)$ as follows:

$$\Phi(x, z, t) = \mathrm{i}\omega\phi(x, z)\exp(\mathrm{i}\omega t) = \mathrm{i}\omega\phi(x)f(z)\exp(\mathrm{i}\omega t). \tag{24}$$

Insertion of Eq. (24) into Eq. (23) gives the two ordinary differential equations

$$\frac{\phi(x),_{xx}}{\phi(x)} = -\frac{f(z),_{zz}}{f(z)} = \left(\frac{m\pi}{L}\right)^2. \tag{25}$$

Therefore, the solution of Eq. (25) can be written by

$$\phi(x, z) = \sum_{m=1}^{M} \xi_m \sin\left(\frac{m\pi x}{L}\right)\cosh\left(\frac{m\pi z}{L}\right). \tag{26}$$

As the liquid displacement and the displacement of the beam must be equal in the case of an absence of a cavitation in the transverse direction at the interface between the liquid and the beam, the compatibility condition at the liquid interface with the beam yields

$$w(x) = \left.\frac{\partial\phi(x, z)}{\partial z}\right|_{z=H}. \tag{27}$$

Substitution of Eqs. (7), (9) and (26) into Eq. (27) gives the following equation:

$$\sum_{m=1}^{M} q_m \sin\left(\frac{m\pi x}{L}\right) = -\sum_{m=1}^{M} \xi_m\left(\frac{m\pi}{L}\right)\sin\left(\frac{m\pi x}{L}\right)\sinh\left(\frac{m\pi H}{L}\right). \tag{28}$$

From Eq. (28), the unknown coefficient of the liquid is given as

$$\xi_m = \frac{-L}{(m\pi)\sinh(m\pi H/L)}\, q_m. \tag{29}$$

Now, it is necessary to evaluate the reference kinetic energies of the liquid to calculate the natural frequencies of the perforated beam in contact with a liquid. The reference kinetic energy of the liquid can be evaluated from its boundary motion [10] as follows:

$$T_L^* = -\tfrac{1}{2}\rho_0 \int_0^L (\partial\phi(x, H)/\partial x)\phi(x, H)\mathrm{d}x, \tag{30}$$

where $\rho_0$ is the mass density of a liquid. To reduce Eq. (30), we insert Eq. (26), (29) into Eq. (30). Therefore the reference kinetic energy of the liquid is written as

$$T_L^* = -\tfrac{1}{2}\rho_0 \int_0^L w(x)\phi(x, H)\,\mathrm{d}x = \tfrac{1}{2}\mathbf{q}^{\mathrm{T}}\mathbf{G}\mathbf{q}, \tag{31}$$

where

$$G_{jk} = \rho_0 U_{jk} \left[ \left( \frac{k\pi}{L} \right) \tanh\left( \frac{k\pi H}{L} \right) \right]^{-1}. \tag{32}$$

The correspondence between the reference kinetic energy of each mode multiplied by its square circular frequency and the maximum potential energy of the same mode is used to find the natural frequencies of the liquid-coupled system. The Rayleigh quotient for the beam in contact with a liquid is given as $V_b/(T_b^* + T_L^*)$. By minimizing the Rayleigh quotient with respect to the unknown parameters $\mathbf{q}$, the following Galerkin equation can be obtained

$$\mathbf{Sq} - \omega^2(\mathbf{Z} + \mathbf{G})\mathbf{q} = \{0\}. \tag{33}$$

The natural frequencies $\omega$ of the perforated beams in contact with a liquid can be calculated by Eq. (33) given an eigenvalue problem.

## 3. Example and discussion

### 3.1. Verification of the analytical method

On the basis of the preceding analysis, the determinant of Eqs. (22) and (33) is numerically solved to find the natural frequencies of the perforated beams with the simply supported boundary condition and the eigenvectors are obtained for the mode shapes by using a mathematical commercial software MathCAD(2000). The number of terms $M$ included in the expansion is set at 100, which gives a converged solution. In order to check the validity and accuracy of the results from the theoretical study, an example is carried out for the liquid-coupled system and the results are compared with the three-dimensional finite elements method analysis results. In the liquid-coupled system as shown in Fig. 2, the thin aluminum beams have a total length of $L = 960$ mm, a width of $b = 120$ mm, and a wall thickness of $h = 5$ mm. The width of the

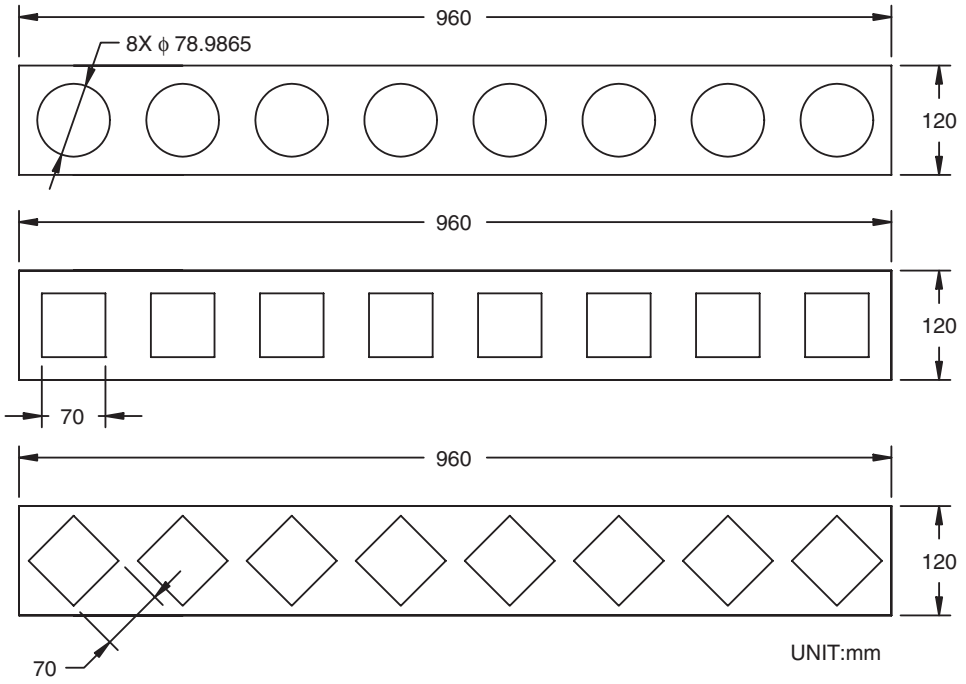


Fig. 2. Example model of the perforated beams.

square and the rotated square holes of the beams is $s = 70\,\text{mm}$, and the diameter of circular holes is $d = 78.9865\,\text{mm}$. Therefore the area of the circular hole is identical to that of the square and the rotated square holes. Each element region of the beams has a width of $a = 120\,\text{mm}$. The material properties of the beams are as follows: modulus of the elasticity $= 69.0\,\text{GPa}$, Poisson's ratio $= 0.3$ and a mass density $= 2700\,\text{kg/m}^3$. Water is assumed as the liquid with a density of $1000\,\text{kg/m}^3$. The depth of the liquid is assumed to be 50 mm. In the finite element model, the three-dimensional liquid domain is assumed to have the same width as the beam and to be laterally bounded by the rigid walls. The perforated beams have eight holes in series, as shown in Fig. 2; three patterns of holes, the square, the rotated square, and the circular holes, are considered. Additionally the natural frequencies and the mode shapes of the solid beam in air and in contact with a liquid are also presented for reference. In the finite element analysis model, the liquid region is divided into a number of liquid elements with eight nodes. On the other hand, we have modeled the perforated beams as deformable shell elements with four nodes. The solid beam is divided into 4608 ($192 \times 24$) elastic shell elements (SHELL63) and the liquid region is divided into three-dimensional contained liquid elements with a number of 27648 ($192 \times 24 \times 6$). For the perforated beams, the division of elements was carried out by an automatic mesh generation with an element size of 5 mm. Finite element analysis by using the commercial computer code ANSYS (version 9.0) was performed to verify the theoretical results for the three patterns of the beam in a dry condition, and for the square pattern in a wet condition. The nodes, which are connected entirely by the liquid elements, are free to move arbitrarily in a three-dimensional space, with the exception of those, which are restricted to a motion in the axial direction along the bottom surface of the liquid cavity. The lateral constraint for the liquid at $y = 0, b$ is a zero displacement in order to impose a two-dimensional beam model. The liquid surface at the holes is imposed to have a zero vertical displacement; this is only an artificial constraint for approximating actual applications. The effects of constraint on the liquid surface at the holes are discussed in Section 3.4. The vertical displacement of the liquid nodes along the wetted beam surface coincides with the corresponding displacement of the beam, which realizes Eq. (27). In the finite element analysis, some torsional modes are detected, but this paper deals with a bending vibration only.

Table 1 shows the natural frequencies of the perforated and the solid beams in air, and it is easy to check the accuracy of the natural frequencies by comparing the theoretical results with the corresponding finite element analysis ones. While the natural frequencies of the solid beam obtained by the theory are underestimated by the finite element analysis results, the natural frequencies of the perforated beams obtained by the theory are slightly overestimated by the finite element analysis results. As can be seen, the results from the perforated beam theory agree quite well with the finite element analysis solution. The largest discrepancy between the theoretical and the FEM results for the perforated beams is 9.8% among the lowest 8 modes, and 9.5% for the solid beam. It is observed that the shape effect of the holes on the natural frequencies in the lower modes is insignificant as shown in Table 1. Fig. 3 shows the dry mode shapes of the perforated beams

Table 1
Natural frequencies of a solid beam and perforated beams with a simply supported boundary condition in air

| Mode | Natural frequency (Hz) | | | | | | | |
|---|---|---|---|---|---|---|---|---|
| | Solid beam | | Perforated beam | | | | | |
| | | | Square holes | | Rotated square holes | | Circular holes | |
| | Theory | ANSYS | Theory | ANSYS | Theory | ANSYS | Theory | ANSYS |
| 1 | 12.4 | 12.5 | 11.7 | 10.7 | 11.5 | 10.4 | 11.4 | 10.9 |
| 2 | 49.8 | 49.9 | 46.7 | 42.8 | 46.1 | 41.7 | 45.6 | 43.8 |
| 3 | 111.9 | 112.7 | 104.6 | 96.4 | 103.7 | 94.3 | 103.0 | 99.0 |
| 4 | 199.0 | 201.1 | 184.4 | 172.0 | 184.8 | 168.8 | 184.1 | 176.9 |
| 5 | 310.9 | 315.3 | 285.9 | 269.7 | 290.1 | 265.8 | 289.8 | 278.1 |
| 6 | 447.7 | 455.6 | 410.3 | 389.7 | 420.4 | 386.2 | 421.2 | 403.5 |
| 7 | 608.4 | 622.0 | 563.3 | 530.5 | 576.5 | 530.9 | 579.7 | 553.4 |
| 8 | 795.9 | 814.5 | 772.9 | 752.6 | 737.7 | 694.4 | 766.6 | 751.8 |

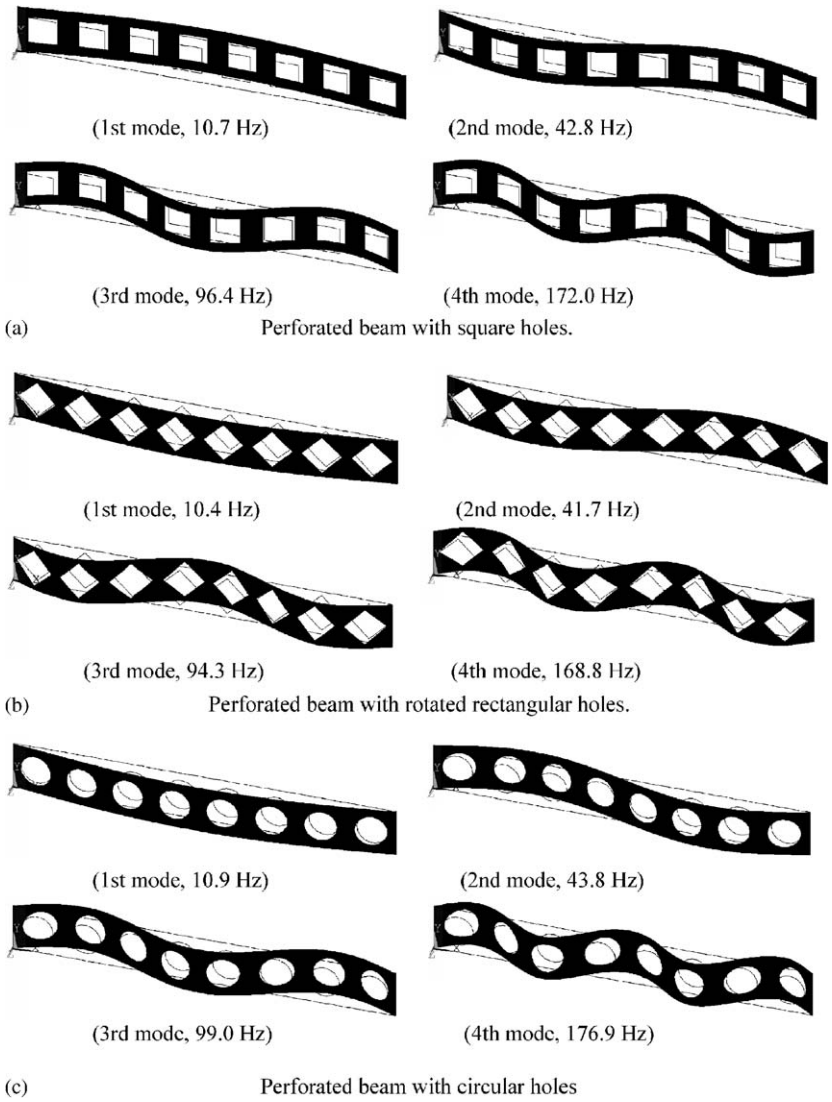


Fig. 3. Bending mode shapes of the perforated beams in air (finite element analysis results).

obtained by using the finite element analysis. Fig. 4 illustrates some deviations of the perforated beam with the square holes from the dry mode shapes of the solid beam obtained by the theory. The mode shapes of the solid beam in air are indicated by dashed lines and the mode shapes of the perforated beam with square holes are delineated by solid lines. Especially, large deviations can be detected in the 6th, 7th, 9th and 10th modes, since the mode shapes cannot coincide with the arrangement of the holes. On the other hand, the 8th mode shape of the perforated beam almost coincides with that of the solid beam because the number of holes is eight. The natural frequencies of the perforated beam in contact with water are listed in Table 2. It is observed that the theoretical natural frequencies of the beam with the square holes agree well to the finite element results within a range of 2.8% deviation for the lowest 8 modes. Fig. 5 shows the wet mode shapes of the perforated beam with square holes computed by using the finite element analysis for the three cases with different constraints. In fact, as a consequence, the liquid has boundary surfaces with a zero pressure at $x = 0$, $L$, but no displacement constrains, therefore a liquid volume change due to a beam vibration is compensated with a liquid movement at the liquid boundary of $x = 0$, $L$.

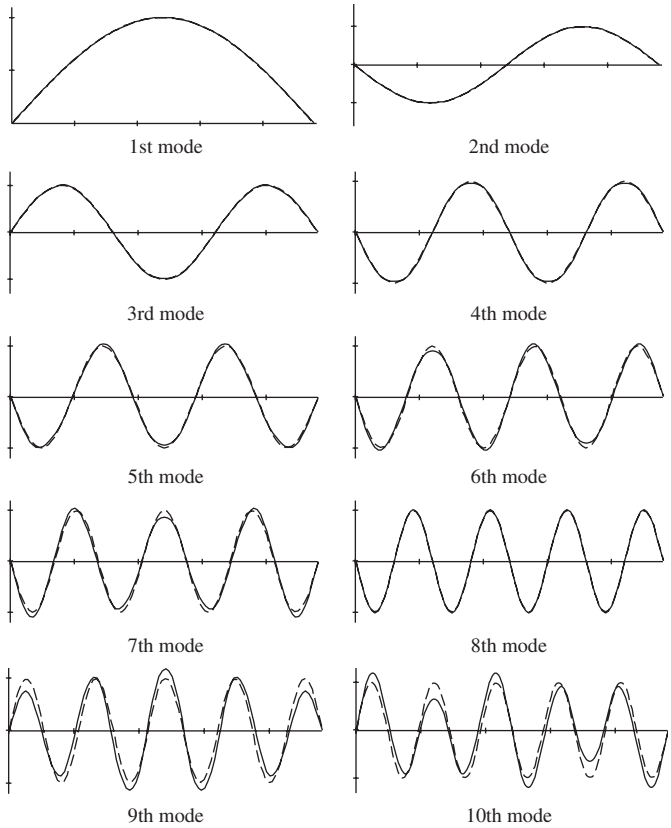


Fig. 4. Theoretical mode shapes of a perforated beam with square holes in air. (———; perforated beam with square holes, – – – – –; solid beam).

Table 2
Natural frequencies of a solid beam and a perforated beam in contact with water

| Mode | Natural frequency (Hz) | | | | | |
|---|---|---|---|---|---|---|
| | Solid beam | | Perforated beam | | | |
| | | | Square holes | | Rotated square holes | Circular holes |
| | Theory | ANSYS | Theory | ANSYS | Theory | Theory |
| 1 | 1.05 | 0.95 | 0.99 | 1.02 | 0.97 | 0.96 |
| 2 | 8.20 | 8.05 | 7.70 | 7.86 | 7.58 | 7.51 |
| 3 | 26.7 | 26.2 | 24.9 | 25.2 | 24.7 | 24.5 |
| 4 | 60.4 | 59.6 | 55.8 | 56.3 | 55.9 | 55.7 |
| 5 | 111.9 | 110.7 | 102.4 | 103.0 | 104.0 | 103.8 |
| 6 | 182.7 | 181.4 | 166.4 | 166.0 | 170.8 | 171.0 |
| 7 | 273.6 | 272.2 | 251.4 | 244.7 | 257.9 | 259.2 |
| 8 | 385.0 | 383.8 | 373.4 | 383.6 | 355.4 | 370.0 |

### 3.2. *Effects of a hole size and shape*

Fig. 6 shows the changes of the normalized natural frequencies of the perforated beam with square holes as a function of the hole size. The normalized natural frequency is defined as the natural frequency of a

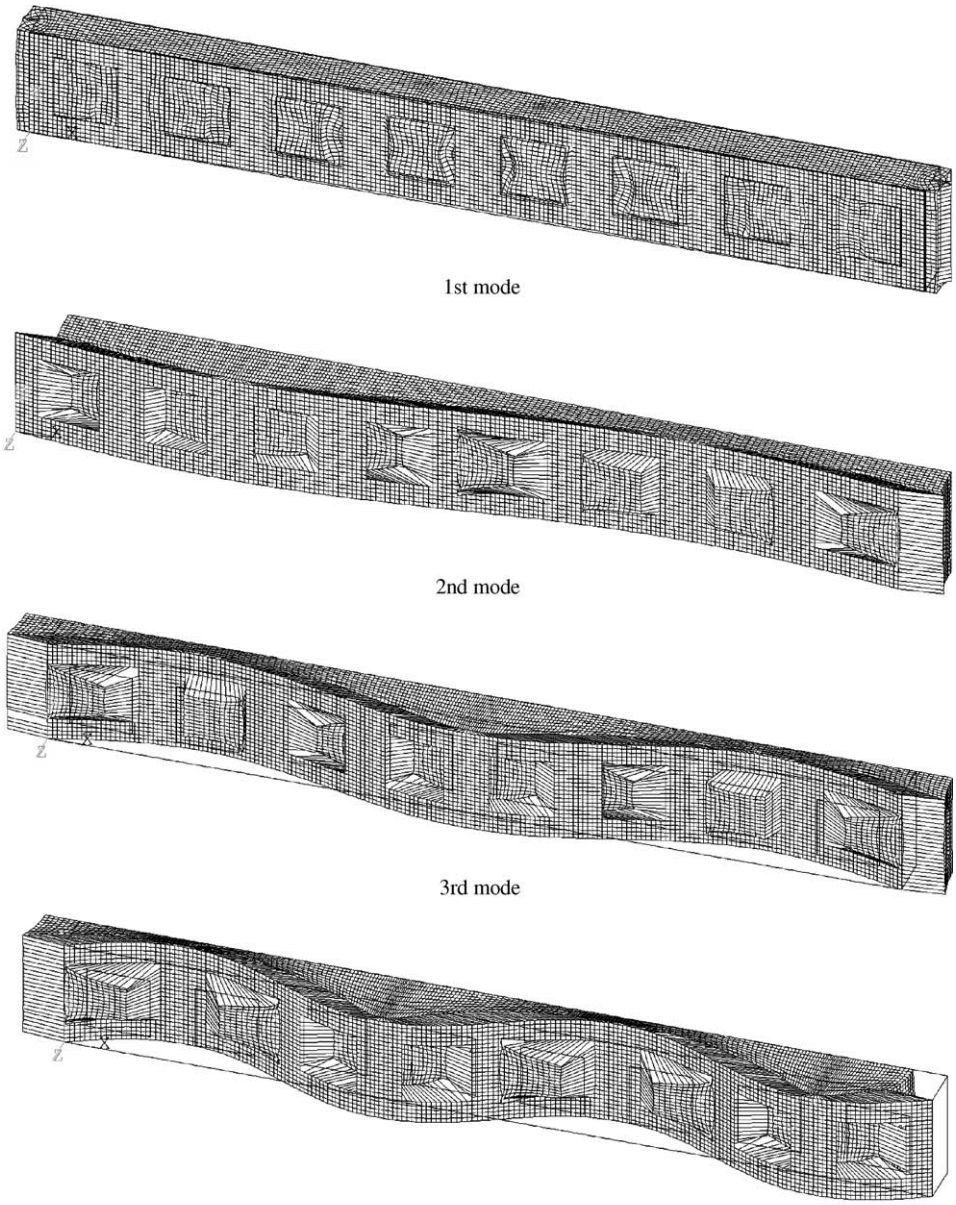


Fig. 5. Wet mode shapes of the perforated beam with square holes (finite element analysis results): (a) vertically constrained case at the liquid surface of the holes, (b) rigid tube inserted case at the holes of the beam and (c) free surface case at the holes of the beam.

perforated beam in air divided by the corresponding natural frequency of a solid beam. The hole size effect of the dry beams on the natural frequencies is not considerable, since the holes of the beams reduce not only the mass but also the stiffness. However, as illustrated in Fig. 6, the normalized natural frequencies are gradually reduced with an increase of the hole size except for the 8th mode, which is a particular case. That is to say, the ligament of the beams corresponds to the antinodes location of the mode shape. Hence, the ligaments with the maximum cross-sectional area bear the maximum bending moments of the beam. Eventually, the stiffness reduction is not considerable when compared with the mass reduction for the 8th mode. For the wet case, the normalized natural frequencies of the perforated beam with square holes in contact with a liquid are illustrated

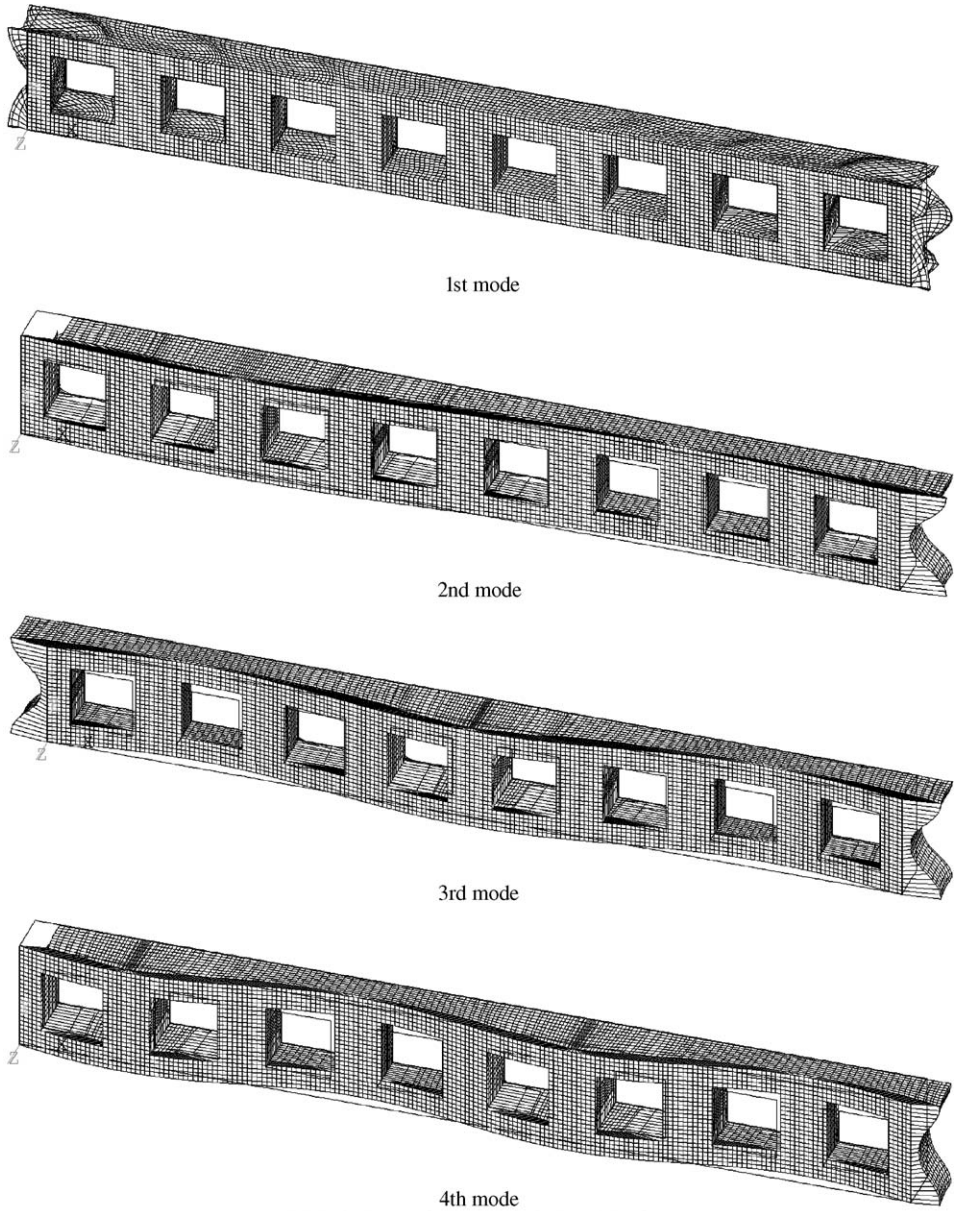


(b) Rigid tube inserted case at the holes of the beam

Fig. 5. (*Continued*)

in Fig. 7 as a function of the hole size. It shows that the normalized natural frequencies of the perforated beam with square holes in contact with a liquid decrease also with the holes size, except for the 8th mode, in the same manner. However, in some cases, the opposite results were observed in an experiment by Jeong et al. [8], because the liquid-contacting area is reduced and it decreases the added mass on the beam. Therefore, it seems that the boundary conditions and the depth of a liquid also considerably affect the wet natural frequencies.

### 3.3. *Effect of a liquid depth*

The effect of a liquid depth on the natural frequencies of a perforated beam in contact with a liquid is investigated here. Fig. 8 shows the normalized natural frequencies obtained by a theoretical calculation, where

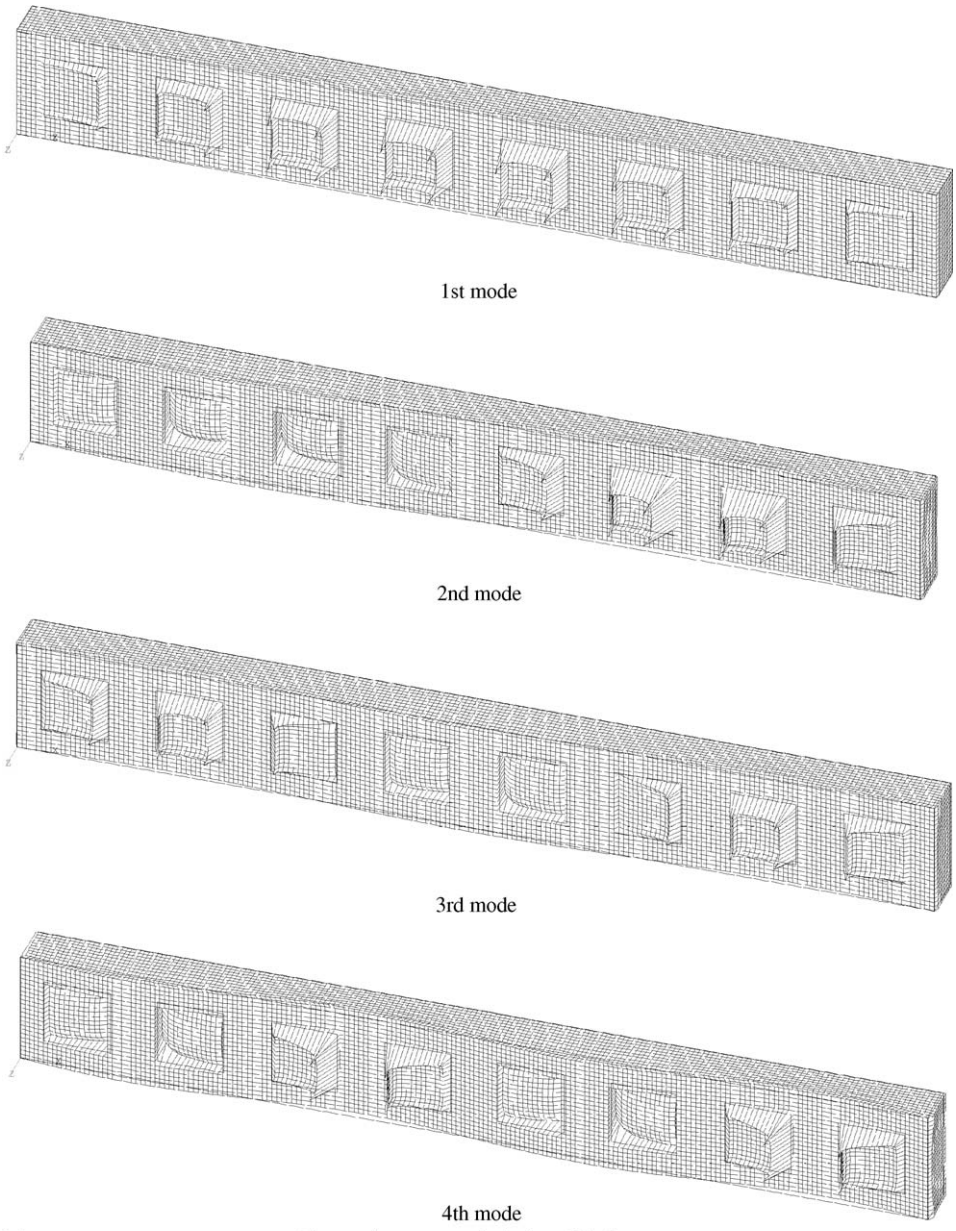


(c) Free surface case at the holes of the beam

Fig. 5. (*Continued*)

a normalization of the natural frequency is carried out with respect to the natural frequency of a perforated beam in contact with water, with an infinite depth. The normalized natural frequency increases with an increase of the liquid depth regardless of the mode numbers. Eventually, the normalized natural frequencies converge to the result of an infinite liquid depth case. The fluid depth reduction significantly affects the coupled natural frequencies when the liquid depth $H$ is small enough, as depicted in Fig. 8. At higher modes, the effect of the liquid depth on the natural frequency is significantly reduced with an increase of the liquid depth, since the liquid at higher modes only moves near the beam. Generally, the reduction of the liquid depth tends to enlarge the hydrodynamic coupling effect and decrease the natural frequencies.

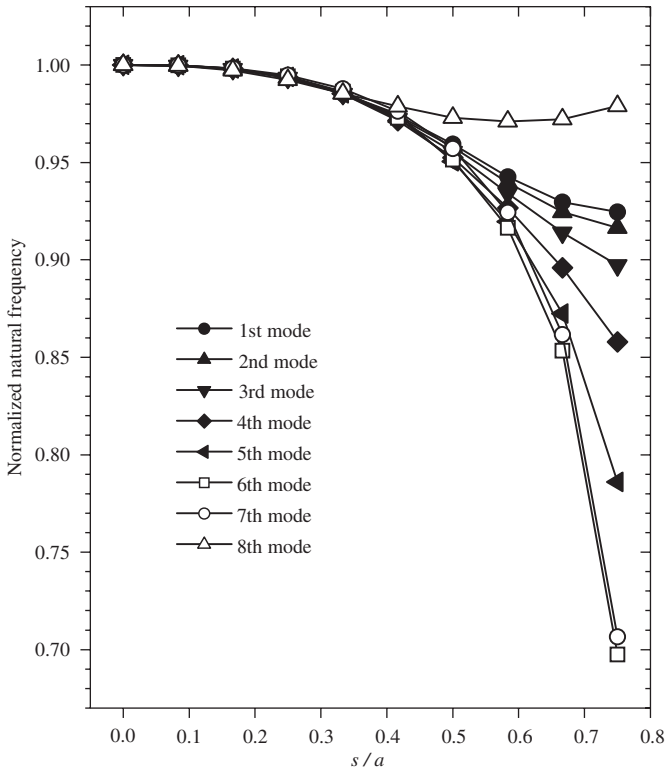


Fig. 6. Hole size effect on the normalized natural frequencies of the perforated beam with square holes in air.

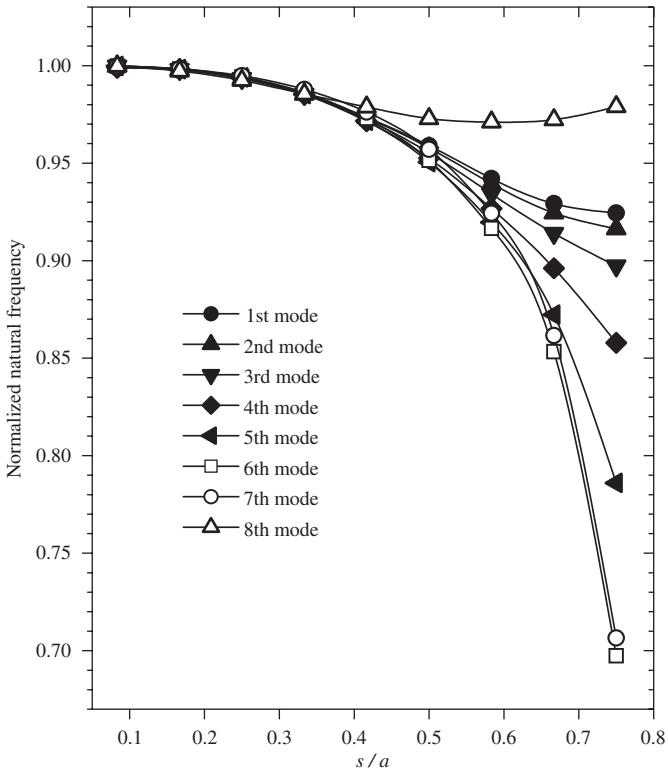


Fig. 7. Hole size effect on the normalized natural frequencies of the perforated beam with square holes in a wet condition.

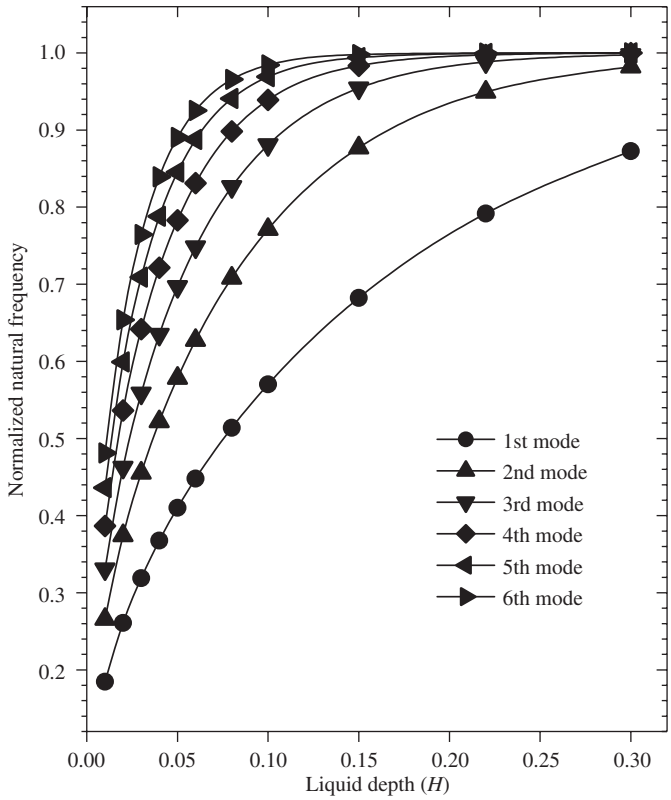


Fig. 8. Water depth effect on the normalized natural frequencies of the perforated beam with square holes.

Table 3
Effect of a liquid constraint at the holes on the natural frequencies of the perforated beam with square holes (finite element analysis results)

| Mode | Natural frequency (Hz) | | |
|---|---|---|---|
| | Vertically constrained case | Rigid tubes inserted case | Free surface case |
| 1 | 1.02 | 0.78 | 5.00 |
| 2 | 7.86 | 5.76 | 19.6 |
| 3 | 25.2 | 18.7 | 45.5 |
| 4 | 56.3 | 42.6 | 83.8 |
| 5 | 103.0 | 79.7 | 135.9 |
| 6 | 166.0 | 130.8 | 202.6 |
| 7 | 244.7 | 193.3 | 282.3 |
| 8 | 383.6 | 372.5 | 446.9 |

### *3.4. Effect of liquid constraints at the holes*

Table 3 shows the changes of the natural frequencies in accordance with different constraints on the liquid at the holes. In the vertically constrained case it is assumed that the liquid at the holes cannot move in the vertical direction but can only move laterally. The rigid tube inserted case simulates the beam penetrated by rigid rectangular tubes in a row; therefore no liquid is presented in the hole area from the top surface to the bottom. As the free surface case indicates that in the case of the perforated beam with free surfaces of the liquid at the holes and without any restrictions at the holes, the liquid can move in any direction. The

constraints at the holes of the beam reveal large differences in the natural frequencies, as depicted in Table 3. It shows that the rigid tubes inserted case has the lowest natural frequencies, since the restriction of the liquid flow due to the rigid tubes increases the hydrodynamic mass during a vibration, and at the same time it increases the length of the liquid flow path. The free surface case has the highest natural frequencies since the hydrodynamic mass is relatively small due to a flow out through the holes of the beam. Unfortunately, it is so complicated that we cannot formulate a theory for these two cases, i.e. for the free surface and the rigid tube inserted cases. Hence, the results of Table 3 are based on the finite element analysis.

## 4. Conclusions

A theoretical study on the free vibration of perforated beams coupled with an ideal liquid is performed. In order to consider the distributed mass and the stiffness of the perforated beams, the Rayleigh–Ritz method is used. The proposed analytical method is verified by the three-dimensional finite element analysis with a good agreement. It is found that the hole size tends to reduce the natural frequencies for all the mode numbers, and the effect of the hole shape on the natural frequencies is insignificant for the dry condition. On the contrary, it is observed that the natural frequencies of the perforated beam in contact with water increase with the hole size because the liquid-contacting area reduction decreases the added mass on the beam. The fluid depth reduction decreases the coupled natural frequencies of the perforated beams when the liquid depth is small enough.

## Acknowledgments

This work was supported by the KOSEF (Korea Science and Engineering Foundation) and CNR (Consiglio Nazionale delle Ricerche) of Italy. Dr. Jeong gratefully acknowledges the financial support of the KOSEF/CNR scientists exchange program for his stay at the University of Parma.

## References

[1] W.J. O'Donnell, B.F. Langer, Design of perforated plates, *Journal of Engineering for Industry—Transactions of the ASME* (1962) 307–318.
[2] W.J. O'Donnell, A study of perforated plates with square penetration patterns, *Welding Research Council Bulletin* 124 (1967) 1089–1101.
[3] W.J. O'Donnell, Further theoretical treatment of perforated plates with square penetration patterns, *Welding Research Council Bulletin* 151 (1970) 1089–1101.
[4] T. Slot, W.J. O'Donnell, Effective elastic constants for thick perforated plates with square and triangular penetration patterns, *Journal of Engineering for Industry—Transactions of the ASME* (1971) 935–942.
[5] W.J. O'Donnell, Effective elastic constants for the bending of thin perforated plates with triangular and square penetration patterns, *Journal of Engineering for Industry—Transactions of the ASME* 95 (1973) 121–128.
[6] D.F. De Santo, Added mass and hydrodynamic damping of perforated plates vibrating in water, *Journal of Pressure Vessel Technology* 103 (1981) 175–182.
[7] K.A. Burgemeister, C.H. Hansen, Calculating resonance frequencies of perforated panels, *Journal of Sound and Vibration* 196 (1996) 387–399.
[8] K.H. Jeong, B.K. Ahn, S.C. Lee, Modal analysis of perforated rectangular plates in contact with water, *Structural Engineering and Mechanics* 12 (2001) 189–200.
[9] J.K. Sinha, S. Singh, A.R. Rao, Added mass and damping of submerged perforated plates, *Journal of Sound and Vibration* 260 (2003) 549–564.
[10] M. Amabili, Eigenvalue problems for vibrating structures coupled with quiescent fluids with free surface, *Journal of Sound and Vibration* 231 (2000) 79–97.